ORIGINAL RESEARCH

Inhibition of SREBP Improves Cardiac Lipidopathy, Improves Endoplasmic Reticulum Stress, and Modulates Chronic Chagas Cardiomyopathy

Janeesh Plakkal Ayyappan, PhD; Kezia Lizardo, DVM; Sean Wang, MD; Edward Yurkow, PhD; Jyothi F. Nagajyothi, PhD

Background—*Trypanosoma cruzi* is an intracellular parasite that causes debilitating chronic Chagas cardiomyopathy (CCM), for which there is no effective drug or vaccine. Previously, we demonstrated increased cardiac lipid accumulation and endoplasmic reticulum stress in mice with CCM. Increased endoplasmic reticulum stress may lead to uncontrolled SREBP (sterol regulatory element-binding protein) activation and lipotoxicity in the myocardium during the intermediate stage of infection and result in progression to chronic CCM. Therefore, we investigated whether inhibiting SREBP activation modulates CCM progression in *T cruzi*–infected mice.

Methods and Results—*T cruzi*–infected cultured cardiomyocytes (3:1 multiplicity of infection; 24 hours postinfection) were incubated with betulin (3 μmol/L per mL), an SREBP inhibitor, for 24 hours. Quantitative polymerase chain reaction and Western blotting analyses demonstrated a significant reduction in SREBP activation, lipid biosynthesis, and endoplasmic reticulum stress in betulin-treated infected cells compared with untreated cells. *T cruzi* infected (10^3 trypomastigotes of the Brazil strain) Swiss mice were fed a customized diet containing betulin during the intermediate stage (40 days postinfection) until the chronic stage (120 DPI). Cardiac ultrasound imaging and histological and biochemical analyses demonstrated anatomical and functional improvements in betulin-treated, infected mice compared with untreated controls: we observed a significant reduction in cholesterol/fatty acid synthesis that may result in the observed cardiac reduction in cardiac lipid accumulation, mitochondrial and endoplasmic reticulum stress, and ventricular enlargement.

Conclusions—Our study (in vitro and vivo) demonstrates that inhibition of cardiac SREBP activation reduces cardiac damage during *T cruzi* infection and modulates CCM in a murine Chagas model. **(*J Am Heart Assoc*. 2020;9:e014255. DOI: 10.1161/JAHA.119.014255.)**

Key Words: betulin • cardiomyopathy • Chagas disease • endoplasmic reticulum stress • mitochondrial stress • SREBP activation

Chagas disease, caused by the parasite *Trypanosoma cruzi*, exists in 2 stages: acute and chronic.[1] During chronic infection, ≈70% of patients remain in an asymptomatic stage without any significant clinical symptoms. However, the remaining 30% develop symptomatic cardiomyopathy, which is a major cause of death and debility in endemic regions. The cellular mechanism(s) and disease pathways involved in the transition from asymptomatic to symptomatic chronic Chagas cardiomyopathy (CCM) are not well understood, and there is thus a lack of potential drug targets. With no vaccines or effective drugs to cure or prevent the progression of cardiomyopathy in chronically infected Chagas patients, the socioeconomic burden remains substantial.[1]

The pathogenesis of CCM is multifactorial and involves aberrant cardiac immunometabolic functions.[1] Previously, using a murine model of CCM, we demonstrated that *T cruzi* invasion during the acute stage of infection causes a dramatic accumulation of intracellular lipids and results in cardiac lipidopathy.[2] This increase in cardiac lipid levels elevates mitochondrial stress, leading to endoplasmic reticulum (ER) stress, and inhibition of ER stress during the asymptomatic (indeterminate) stage of infection modulates CCM.[3] Chronic ER stress may deregulate expression of SREBPs (sterol regulatory element-binding proteins) and elevate intracellular

From the Department of Microbiology, Biochemistry and Molecular Genetics, Public Health Research Institute, New Jersey Medical School, Newark, NJ (J.P.A., K.L., J.F.N.); and Rutgers Molecular Imaging Center, Piscataway, NJ (S.W., E.Y.).

Accompanying Figure S1 through S3 are available at https://www.ahajournals.org/doi/suppl/10.1161/JAHA.119.014255

Correspondence to: Jyothi F. Nagajyothi, PhD, 225 Warren St, Newark, NJ 07103. E-mail: jfn31@njms.rutgers.edu

Received August 9, 2019; accepted December 5, 2019.

Clinical Perspective

What Is New?

- In a murine model of Chagas cardiomyopathy, there is an increase in SREBP (sterol regulatory element-binding protein) activation.
- SREBP activation may be a novel mechanism by which Chagas cardiomyopathy can be modulated.

What Are the Clinical Implications?

- Cardiac lipid accumulation-induced mitochondrial oxidative stress and endoplasmic reticulum stress may result in cardiomyopathy in chronic Chagas disease.
- Prevention of cardiac lipid accumulation by inhibiting cardiac SREBP activation at the early stage of chronic infection may be an effective strategy to prevent the progression of Chagas cardiomyopathy.

lipid levels.[4] Consistent with this, we detected a significant amount of lipids in cardiac sections of a patient with CCM compared with ischemic heart sections.[2] These data suggest that irregular SREBP signaling during the indeterminate stage of *T cruzi* infection may form a vicious cycle, with mitochondrial and ER stress leading to cardiolipidopathy that could influence CCM progression.

To test this, in the present study, we investigated whether SREBP activation plays a major role in inducing ER stress and CCM progression using a murine model of Chagas disease and betulin, an inhibitor of SREBP processing. Betulin is a naturally occurring triterpene commonly isolated from the bark of birch trees.[5] Betulin inhibits the maturation of SREBPs and decreases the biosynthesis of cholesterol and fatty acids.[5] Betulin inhibits SREBP maturation by binding to SCAP (SREBP cleavage-activating protein) (SREBP chaperone) and promoting the interaction between SCAP and insulin-induced gene 1 (Insig1), which leads to the ER retention of SREBP. We treated *T cruzi*–infected mice with betulin (customized diet) during the indeterminate stage and evaluated its effect on CCM progression in the chronic stage. CD1 mice infected with a low dose of *T cruzi* generally display low parasitemia and proinflammatory signaling (acute infection, 15–30 days postinfection [DPI]) and develop cardiomyopathy after ≈90 DPI. Parasitemia and proinflammatory signaling were mostly absent in these mice during the late acute phase and, thus, between 40 and 70 DPI was considered an indeterminate stage of infection in murine Chagas disease (CD) models.[6,7] Our results show that betulin treatment during the indeterminate stage significantly improved cardiac functions and ameliorated *T cruzi* infection–induced CCM. We demonstrated that betulin treatment reduced cardiac lipid accumulation, reduced mitochondrial and ER stress, and prevented ventricular enlargement in *T cruzi*–infected mice. Supporting the in vivo studies, we also demonstrated that betulin could reduce ER stress in *T cruzi*–infected cultured cardiomyocytes.

Materials and Methods

The authors declare that all supporting data are available within the article (and its online supplementary files).

Animal Ethics Statement

All experimental animal protocols were approved by the Institutional Animal Care and Use and Institutional Biosafety Committees of Rutgers University and adhere to the National Research Council guidelines.

Animal Model and Experimental Design

The Brazil strain of *T cruzi* (DTU1, 21) was maintained by passage in C3H/Hej mice (Jackson Laboratories, Bar Harbor, ME).[1] Male Swiss CD1 mice have been known to develop CCM, which was inversely related to body fat mass.[8] Also, body fat mass distribution differs between male and female. Therefore, we have used only male mice in our studies. CD1 mice (Jackson Laboratories; n=50) were infected intraperitoneally (n=30, expecting 35% mortality during acute stage) at 6 to 7 weeks of age with 10^3 trypomastigotes of the Brazil strain and fed a Formulab diet No. 5008. Mice were maintained on a 12-hour light/dark cycle. After 40 DPI, one set of infected mice (n=10; randomly selected) was fed a betulin-containing diet (30 mg betulin/kg diet). One set of uninfected mice (n=10) was also fed a betulin-containing diet. Uninfected control regular diet (Formulab diet No. 5008) fed mice were used as control mice. All the mice (n=10/group) were euthanized at 120 DPI after cardiac imaging analysis, and blood, heart, and liver samples were collected. Portions of the harvested tissues were fixed in 10% formalin for histological analysis. Portions of tissues were also stored immediately at −80°C for total RNA isolation and protein extraction. The experiment was repeated using the same number of mice. A flowchart describing the experimental design is presented as Figure S1A.

In vitro T cruzi infection

The rat-derived H9c2 cardiomyoblast cells (CRL-1446) were purchased from American Type Culture Collection (ATCC Cell Biology Collection). Cell cultures were routinely maintained in DMEM (Gibco), containing 2 mmol/L L-glutamine and 1.5 g/L sodium bicarbonate and supplemented with 10% fetal bovine serum (Gibco) at 37°C in a 5% CO_2 atmosphere. H9c2 cells were infected by trypomastigotes (Brazil strain) at a multiplicity of infection of 3:1. After 24 hours postinfection

(hpi), infected cells were washed to remove unbound parasites, and to one set of uninfected and infected cells, betulin, 3 μmol/L per mL medium (1.9 μL dissolved in dimethyl sulfoxide), was added and incubated for another 24 hours. Dimethyl sulfoxide (1.9 μL/mL medium) was added to another set of infected and uninfected cells. Cells were harvested at 48 hpi for protein and mRNA analysis. The experiment was repeated with n=3/group (Figure S1B).

Immunoblot analysis

Heart lysates were prepared as previously described.[6] An aliquot of each sample (30 μg protein) was subjected to SDS-PAGE, and the proteins were transferred to nitrocellulose filters for immunoblot analysis. CHOP (CCAAT-enhancer–binding protein)–specific mouse monoclonal antibody (1:1000 dilution; L63F7; Cell Signaling), BIP (binding immunoglobulin protein)–specific rabbit monoclonal antibody (1:1000 dilution; C50B12; Cell Signaling), phosphorylated perilipin-specific mouse monoclonal antibody (1:1000 dilution; 4856; Vala Sciences), low-density lipoprotein (LDL)–specific chicken polyclonal antibody (1:1000 dilution; PA1-31260; Cell Signaling), SREBP-1–specific rabbit polyclonal antibody (1:1000 dilution; AB28481; Abcam), peroxisome proliferator-activated receptor (PPAR)-α–specific mouse monoclonal antibody (1:1000 dilution; MA1-822; Thermoscientific), adiponectin-specific mouse monoclonal antibody (1:1000 dilution; AB22554; Abcam), ABCA1 (ATP-binding cassette transporter)–specific mouse monoclonal antibody (1:500 dilution; AB.H10; Abcam), fatty acid synthase–specific rabbit monoclonal antibody (1:1000 dilution; C20G5; Cell Signaling), UCP3 (uncoupling protein 3)-specific rabbit monoclonal antibody (1:1000 dilution; D6J8K; Cell Signaling), tumor necrosis factor (TNF)-α–specific rabbit polyclonal antibody (1:2000 dilution; AB6671; Abcam), and interferon-γ–specific rabbit monoclonal antibody (1:1000 dilution; EPR1108; Abcam) were used as primary antisera. Horseradish peroxidase–conjugated goat anti-mouse immunoglobulin (1:2000 dilution; Thermo Scientific) or horseradish peroxidase–conjugated goat anti-rabbit immunoglobulin (1:2000 dilution; Thermo Scientific) was used to detect specific protein bands (explained in figure legends) using a chemiluminescence system.[9] GDI (Guanosine nucleotide dissociation inhibitor) (1:10 000 dilution; 71-0300; and rabbit polyclonal; Invitrogen, Carlsbad, CA) and a secondary antibody horseradish peroxidase–conjugated goat anti-rabbit (1:2000 dilution; Amersham Biosciences) were used to normalize protein loading.

Real-time polymerase chain reaction quantification

Total RNA from the hearts of *T cruzi*–infected and uninfected mice, fed either a control diet or a betulin diet, was isolated using the Trizol reagent at 120 DPI (Invitrogen). Isolated RNA was purified, quantitated, and reverse transcribed, as described earlier.[3] A quantitative polymerase chain reaction (qPCR) analysis was performed using Power SYBR Green PCR Master Mix (Thermo Fisher Scientific) to measure the mRNA levels of adiponectin, PPAR-γ, SREBP-1, SREBP-2, SCAP, FAS (fatty acid synthase), hydroxymethylglutaryl–coenzyme A (HMG-CoA) synthase, HMG-CoA reductase, IDOL (increased degradation of LDL receptor protein), apolipoprotein E, apolipoprotein B, LDL receptor, TNF-α, interleukin-6, interleukin-10, and hypoxanthine-guanine phosphoribosyltransferase genes, following the manufacturer's protocol. The murine-specific primers used to amplify the above genes are listed in Table. To normalize gene expression and calculate fold change, mRNA expression of the housekeeping gene hypoxanthine-guanine phosphoribosyltransferase was measured. For each sample, both the housekeeping and target genes were amplified in triplicate.

Histological analyses

Freshly isolated tissues were fixed with phosphate-buffered formalin for a minimum of 48 hours and then embedded in paraffin wax. Hematoxylin and eosin and Masson chrome staining were performed, and the images were captured as previously published.[6] Filipin staining was performed to analyze free cholesterol levels in the optimal cutting temperature (OCT) compound-embedded heart sections, as previously described.[2]

Immunofluorescence analyses were performed on the frozen heart sections using anti-LDL (1:250 dilution), and the images were captured as previously described.[10] The fluorescent intensities of the images were quantified using the National Institutes of Health Image J program for 4 to 6 images of each heart. Immunohistochemical analysis was performed on the formalin-fixed heart using TNF-α–specific rabbit polyclonal antibody (1:250 dilution; AB6671; Abcam), as described earlier.[8]

Cardiac ultrasound analysis

Cardiac ultrasound imaging of the mice was performed at 100 DPI (chronic stage of infection) using a Vevo 2100 ultra-high-frequency ultrasound system (Visual Sonics Inc, Toronto, Canada) at the Rutgers University Molecular Imaging Center, as described earlier (n=5/group).[3] Doppler ultrasound capabilities of the system were also used to determine the blood flow velocities of the aorta and pulmonary arteries as well as to profile mitral valve function.[3] B-mode, M-mode, and pulse wave Doppler image files were collected from both the parasternal long-axis and short-axis views. Morphometric measurements and blood flow velocity of major vessels and valves were determined using image analysis tools available in the Vevo workstation software.

Statistical Analysis

For immunoblotting analysis (n=5), the densitometric values of the immunoreactive bands (immunoblotting) were analyzed

Table. Primer Sequences Used for Real-Time PCR

Primer Name	Forward (5′–3′)	Reverse (3′–5′)
BIP	GGTGCAGCAGGACATCAAGTT	CCCACCTCCAATATCAACTTGA
CHOP	CTGCCTTTCACCTTGGAGAC	CGTTTCCTGGGGATGAGATA
TNF-α	CCCTCACACTCAGATCATCTTCT	GCTACGACGTGGGCTACAG
SREBP-1A	GGCCGAGATGTGCGAACT	TTGTTGATGAGCTGGAGCATGT
SREBP-1C	GGAGCCATGGATTGCACATT	GGCCCGGGAAGTCACTGT
SREBP-2	GCGTTCTGGAGACCATGGA	ACAAAGTTGCTCTGAAAACAAATCA
SCAP	ATTTGCTCACCGTGGAGATGTT	GAAGTCATCCAGGCCACTACTAATG
S1P	TGCTCCCACCTGACTTTGAAG	GCTGTGAAGTATCCGTTGAAAGC
INSIG-1	TCACAGTGACTGAGCTTCAGCA	TCATCTTCATCACACCCAGGAC
FAS	GCTGCGGAAACTTCAGGAAAT	AGAGACGTGTCACTCCTGGACTT
Acetyl CoA carboxylase	TGACAGACTGATCGCAGAGAAAG	TGGAGAGCCCCACACACA
Adiponectin	GTTGCAAGCTCTCCTGTTCC	TCTCCAGGAGTGCCATCTCT
HMG-CoA synthase	GCCGTGAACTGGGTCGAA	GCATATATAGCAATGTCTCCTGCAA
HMG-CoA reductase	CTTGTGGAATGCCTTGTGATTG	AGCCGAAGCAGCACATGAT
LDL receptor	AGGCTGTGGGCTCCATAGG	TGCGGTCCAGGGTCATCT
Glucokinase	CCGTGATCCGGGAAGAGAA	GGGAAACCTGACAGGGATGAG
ATP citrate lyase	GCCAGCGGGAGCACATC	CTTTGCAGGTGCCACTTCATC
Squalene synthase	CCAACTCAATGGGTCTGTTCCT	TGGCTTAGCAAAGTCTTCCAACT
IDOL	CGAGCCATCACCGAAACAC	CGCGACTGTACTGCATCATGA
ABCA1	CGTTTCCGGGAAGTGTCCTA	GCTAGAGATGACAAGGAGGATGGA
Apolipoprotein E	GCAGGCGGAGATCTTCCA	CCACTGGCGATGCATGTC
Interferon-γ	AGCGGCTGACTGAACTCAGATTGTAG	GTCACAGTTTTCAGCTGTATAGGG
HPRT	GTTGGATCAAGGCCAGACTTTGTT	GAGGGTAGGCTGGCCTATAGGCT

ABCA1 indicates ATP-binding cassette transporter; BIP, binding immunoglobulin protein; CHOP, CCAAT-enhancer–binding protein; CoA, coenzyme A; FAS, fatty acid synthase; HMG-CoA, hydroxymethylglutaryl-CoA; HPRT, hypoxanthine-guanine phosphoribosyltransferase; IDOL, increased degradation of LDL receptor protein; INSIG-1, insulin-induced gene 1; LDL, low-density lipoprotein; SCAP, SREBP cleavage-activating protein; S1P, site-1 protease; SREBP, sterol regulatory element-binding protein; TNF-α, tumor necrosis factor-α.

with the Image Studio lite package V5.2 (LI-COR Biosciences, Lincoln, NE). Statistical analyses were performed using a Student *t* test (Microsoft Excel), as appropriate, to compare between 2 groups. The results were expressed as means±SEs. All analyses were performed using $P<0.05$ for statistical significance. Immunoblot, immunofluorescence, and quantification of mRNA levels (taken the average to calculate *P* value) were performed at least 3 times, and representative data are presented in the figures.

Results

Betulin Treatment Decreases *T cruzi* Infection–Induced Fatty Acid Metabolism by Inhibiting SREBP Activation in Cultured Cardiomyocytes

We analyzed the levels of SREBP and associated, downstream FASs (acetyl CoA carboxylase and ATP citrate lyase) in infected cardiomyocytes compared with uninfected cells by immunoblotting analysis at 48 hpi and found that *T cruzi* infection significantly increased the levels of all these proteins (Figure 1). This increase was inhibited by incubating the *T cruzi*–infected cardiomyocytes (24 hpi) with 3 μmol/L per mL betulin (Figure 1). Thus, *T cruzi* infection induces SREBP levels and activates downstream fatty acid metabolism, which can be inhibited by betulin treatment. We further analyzed mRNA levels of SREBPs and downstream SREBP-regulated genes, including *SREBP-1A*, *SREBP-1C*, *SREBP-2*, *SCAP*, *site-1 protease*, and *INSIG-1*, in *T cruzi*–infected cells treated with and without betulin and compared with uninfected control cells at 48 hpi. qPCR analysis demonstrated a significant increase in the levels of all these genes in infected cells, which was again inhibited by betulin treatment (Figure S2A). qPCR analysis also demonstrated that *T cruzi* infection induces expression of genes involved in fatty acid and cholesterol metabolism, specifically such as *FAS*, *acetyl CoA carboxylase*, *acetyl CoA*

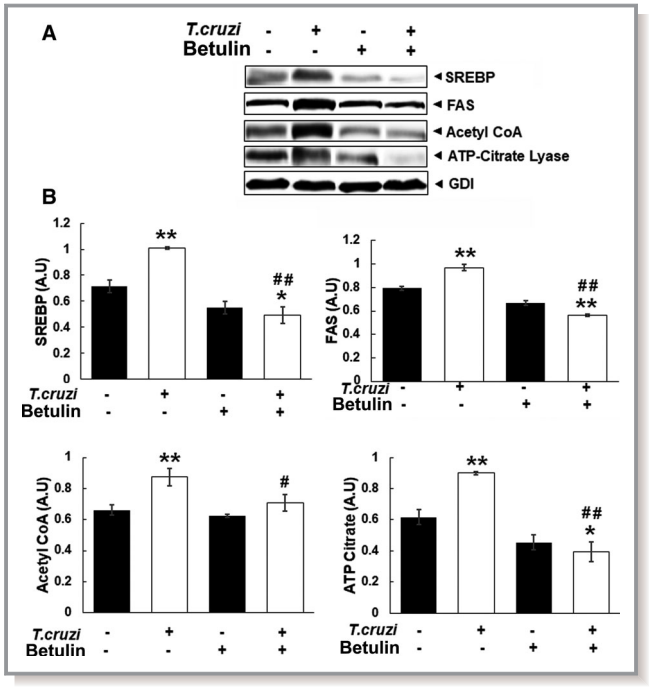

Figure 1. Effect of SREBP (sterol regulatory element-binding protein) inhibitor (betulin) on SREBP and fatty acid metabolism in cardiomyocytes infected with *Trypanosoma cruzi*. **A**, Immunoblot analysis showing the levels of SREBP, FAS (fatty acid synthase), acetyl CoA carboxylase, and ATP–citrate lyase proteins in *T cruzi*–infected or uninfected H9c2 cells treated or left untreated with SREBP inhibitor. **B**, Bar graph depicting fold changes in protein levels of SREBP, FAS, acetyl CoA carboxylase, and ATP–citrate lyase normalized to GDI (guanosine nucleotide dissociation inhibitor) expression. The error bars represent SEM. A.U. indicates arbitrary unit. $^{*}P\leq0.05$ or $^{**}P\leq0.01$ compared with uninfected untreated. $^{\#}P\leq0.05$ or $^{\#\#}P\leq0.01$ compared with infected untreated.

synthase, *adiponectin HMG-CoA*, and *LDL,* which was also inhibited by betulin treatment (Figure S2B). Overall, these data reveal that the increase in intracellular de novo synthesis of fatty acids and cholesterol induced by *T cruzi* infection can be inhibited by blocking SREBP activation in vitro.

Inhibition of SREBP Activation Reduces *T cruzi* Infection–Induced ER Stress in Cultured Cardiomyocytes

Cultured cardiomyocytes infected with *T cruzi* demonstrated significantly increased protein levels of the ER stress markers BIP, CHOP, and PDI (1.5-, 4-, and 2-fold, respectively) compared with uninfected cells at 48 hpi (Figure 2). This increase was inhibited by betulin treatment (3 µmol/L per mL added after 24 hpi), specifically in *T cruzi*–infected cells (≈2-fold compared with untreated infected cells at 48 hpi) (Figure 2). Thus, *T cruzi* infection also induces ER stress in cardiomyocytes, which is ameliorated by inhibition of SREBP activation.

Betulin Treatment of Infected Mice During the Indeterminate Stage Modulates Cardiac Morphological Characteristics and Function at the Chronic Stage

Ultrasound imaging analysis of the hearts of *T cruzi*–infected mice using Vevo2100 demonstrated significant changes in cardiac morphological characteristics and function compared with uninfected mice at 120 DPI (Figure 3A). Specifically, *T cruzi* infection caused a significant decrease in the left ventricle internal diameter at end systole and an increase in the right ventricle internal diameter at end diastole and systole compared with uninfected mice. Notably, infected mice fed a betulin diet significantly improved both LVID and RVID compared with infected mice fed a regular diet (Figure 3A).

Treatment With Betulin Improves Myocardial Pathological Characteristics in Chronic *T cruzi*–Infected Mice

Histological analyses of heart sections by hematoxylin and eosin staining demonstrated increased levels of infiltrated immune cells (black arrow), degenerating muscle fibers (arrowhead), and vasculitis predominantly in right ventricles of infected mice compared with in uninfected mice (Figure 3B). Masson trichrome–stained sections demonstrated increased fibrosis in the myocardium of the infected mice compared with uninfected mice (Figure 3C). Betulin treatment alleviated this cardiac pathological condition and the presence of preserved cardiomyocytes compared with infected untreated mice (Figure 3B and 3C).

Treatment With Betulin Improves Cardiac Lipid Metabolism and Reduces Cardiac Lipid Accumulation in *T cruzi*–Infected Chronic Mice

Our in vitro studies demonstrated that *T cruzi* infection induces SREBP activation and increases lipid metabolism and that inhibition of SREBP activation during infection reduces this infection-induced lipid biosynthesis (Figure 1). Consistent with these in vitro studies, the hearts of *T cruzi*–infected mice showed significantly elevated levels of SREBP (1.5-fold) compared with uninfected mice, as demonstrated by immunoblotting analysis at 120 DPI (Figure 4A and B). In contrast, infected mice fed a betulin diet showed significantly decreased cardiac SREBP levels (4-fold) compared with infected mice fed a regular diet at 120 DPI (Figure 4A and B). The increased SREBP levels in the hearts of *T cruzi*–infected mice were associated with significantly elevated protein levels of LDL, FAS, and acetyl CoA carboxylase

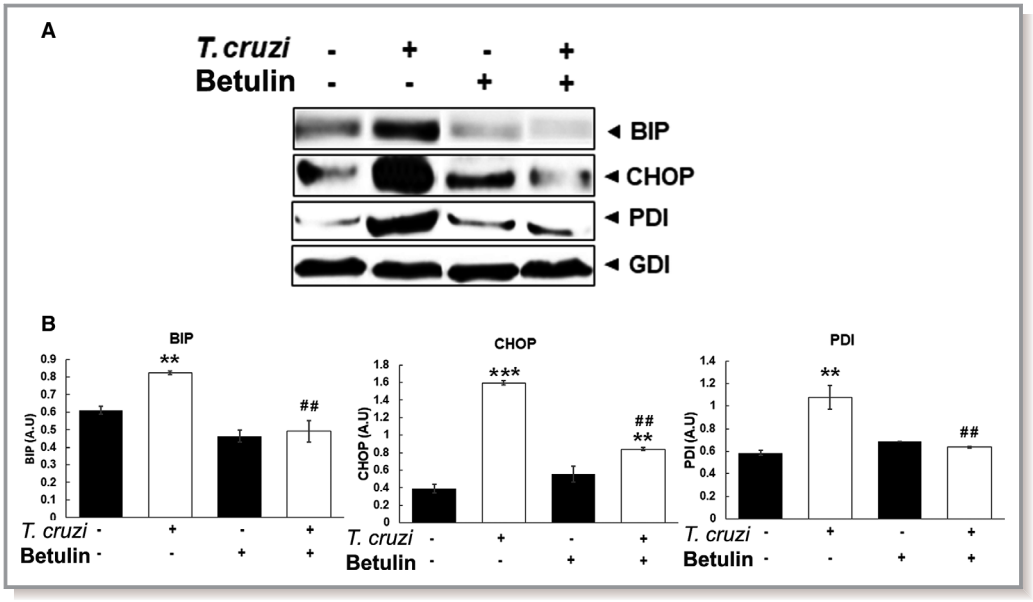

Figure 2. Effect of SREBP (sterol regulatory element-binding protein inhibitor (betulin) on endoplasmic reticulum (ER) stress proteins in cardiomyocytes infected with *Trypanosoma cruzi*. **A**, Immunoblot analysis showing the levels of ER stress markers BIP (binding immunoglobulin protein), CHOP (CCAAT-enhancer–binding protein), and PDI (protein disulfide isomerase) protein in *T cruzi*–infected or uninfected H9c2 cells treated or left untreated with the SREBP inhibitor. **B**, Bar graph depicting fold changes in the protein levels of BIP, CHOP, and PDI normalized to GDI (guanosine nucleotide dissociation inhibitor) expression. The error bars represent SEM. A.U. indicates arbitrary unit. $^{**}P\leq0.01$ or $^{***}P\leq0.001$ compared with uninfected untreated. $^{\#\#}P\leq0.01$ compared with infected untreated.

(2.5-, 3-, and 1.5-fold, respectively) compared with uninfected mice (Figure 4A and B). *T cruzi* infection also increased lipid catabolism, as shown by a significant increase (5-fold compared with uninfected mice) in the levels of phosphorylated perilipin and PPAR-α, which are involved in lipolysis and lipid oxidation, respectively, at 120 DPI (Figure 4C and D). Treatment with betulin during the indeterminate stage of infection significantly reduced the levels of the cardiac lipids LDL, FAS, and acetyl CoA carboxylase compared with untreated infected mice at 120 DPI. Betulin treatment also significantly increased the cardiac levels of ABCA1 in infected mice compared with untreated infected mice, suggesting improved cholesterol efflux (Figure 4C and D). Immunofluorescence analysis also demonstrated an increase in cardiac LDL and cholesterol during infection, which were both decreased by betulin treatment (Figure 5A and B).

Furthermore, we also analyzed mRNA levels of several essential genes involved in lipid metabolism induced by SREBP transcriptional activation during chronic *T cruzi* infection. qPCR analysis demonstrated a significant increase in the mRNA levels of genes involved in SREBP activation, such as *SREBP 1A*, *SREBP 2*, *SCAP*, and *site-1 protease*, in the hearts of infected mice at 120 DPI, which were significantly decreased on betulin treatment (Figure S3A). mRNA levels of genes involved in fatty acid biosynthesis, such as *FAS*, *glucokinase*, *ATP citrate lyase*, and *acetyl CoA synthase*, also significantly increased in the hearts of infected mice, which were significantly decreased on betulin treatment (Figure S3B). These data suggest that betulin reduces *T cruzi* infection–induced SREBP activation and de novo fatty acid biosynthesis in the heart and modulates cardiac lipid load during infection. We also analyzed the mRNA levels of genes involved in cholesterol biosynthesis and cholesterol efflux (Figure S3C). qPCR analysis demonstrated significantly increased levels of the cholesterol biosynthesis genes *HMG-CoA synthase*, *farnesyl diphosphate synthase*, and *squalene synthase*, and decreased levels of the cholesterol efflux–related genes *ABCA1* and *APOE*, in the hearts of infected mice compared with uninfected mice. This suggests that *T cruzi* infection increases cholesterol biosynthesis and inhibits cholesterol efflux in the hearts during indeterminate and chronic stages of infection. Interestingly, the mRNA levels of HMG-CoA synthase, farnesyl diphosphate synthase, and squalene synthase significantly decreased, and ABCA1 and APOE significantly increased, in the hearts of infected betulin-treated mice compared with untreated infected mice at 120 DPI (Figure S3C). Overall, this qPCR analysis demonstrated that inhibition of SREBP activation significantly reduces cardiac lipid biosynthesis and lipid metabolism and improves cholesterol efflux during chronic stages of *T cruzi* infection.

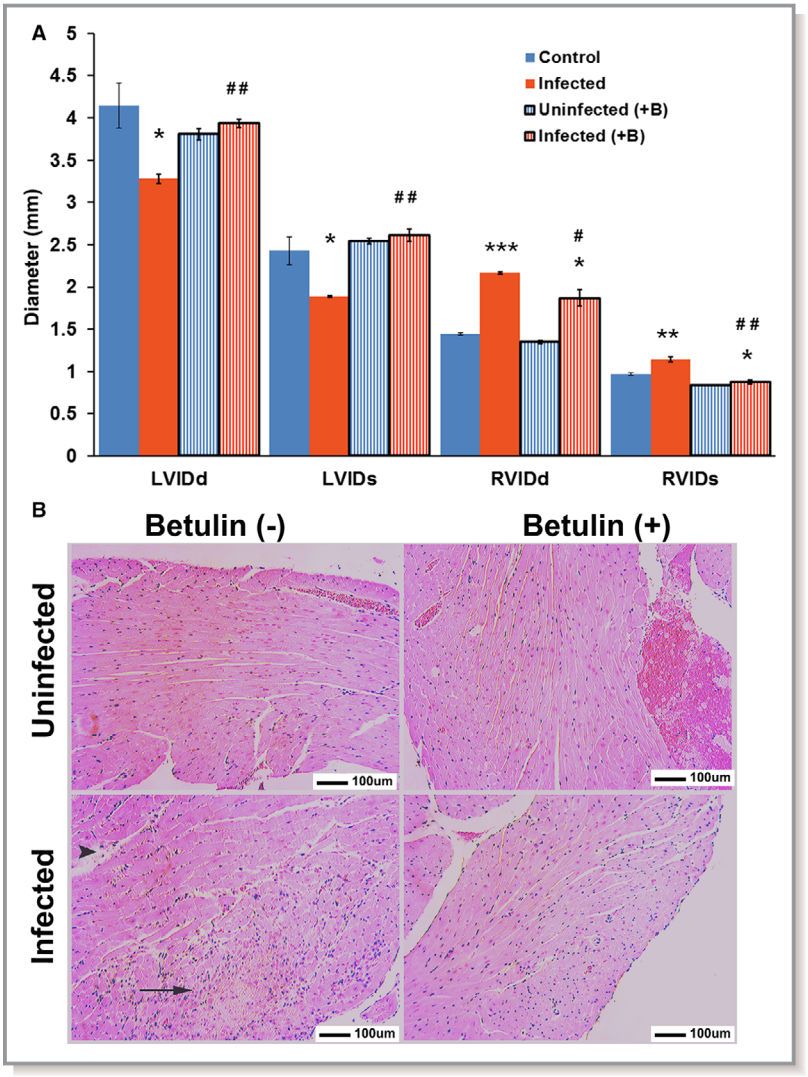

Figure 3. Amelioration of myocardial damage by SREBP (sterol regulatory element-binding protein) inhibitor in mice during chronic infection at 120 days postinfection (DPI) (n=8; minimum 5 images/section were analyzed). **A**, Left ventricle internal diameter (LVID) and right ventricle internal diameter (RVID), measured by ultrasound analysis of the hearts both at diastole (d) and systole (s) conditions at 120 DPI, in infected or uninfected mice, treated or untreated with SREBP inhibitor (betulin [+B]), as indicated. **B**, Hematoxylin and eosin staining of hearts in indicated mice. Inflammation, long black arrow; fibrosis, red arrowhead; degenerating cardiac muscle fiber, black arrowhead (see Figure S3); and presence of adipocytes or lipid granules, red long arrow (see Figure S3). Bar=100 μm. Additional images are presented as Figure S3. **C**, Photomicrographs of Masson trichrome–stained heart sections demonstrating cardiac fibrosis and collagen deposition. Bar=100 μm. The error bars represent SEM. $^{*}P\leq0.05$, $^{**}P\leq0.01$, or $^{***}P\leq0.001$ compared with uninfected untreated mice. $^{\#}P\leq0.05$ or $^{\#\#}P\leq0.01$ compared with infected untreated mice.

Inhibition of SREBP Activation During the Indeterminate Stage of Infection Improves Cardiac Mitochondrial Functions and Reduces Cardiac ER Stress and Inflammation

Immunoblot analysis demonstrated a significant decrease in the cardiac levels of proteins involved in mitochondrial functions, including cytochrome C, HSP (heat shock protein) 60, COX IV (cytochrome oxidase IV), and SDHA (succinate dehydrogenase complex subunit) (3-, 2-, 2-, and 2.2-fold, respectively) compared with uninfected mice (Figure 6A). In contrast, mice fed a betulin diet displayed significantly increased levels of cytochrome C, HSP-60, COX IV, and SDHA (2-, 1.5-, 1.5-, and 2-fold, respectively) in the hearts of

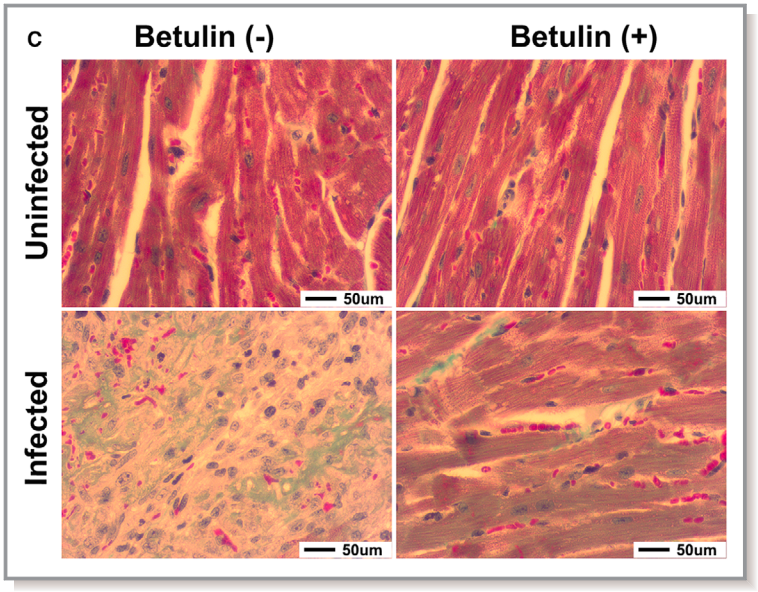

Figure 3. Continued

infected mice compared with untreated infected mice at 120 DPI, suggesting that inhibition of SREBP activation improves cardiac mitochondrial functions. Immunoblot analysis demonstrated a significant increase in the levels of ER stress markers, such as BIP and CHOP (1.5- and 7-fold, respectively), in the hearts of infected mice compared with

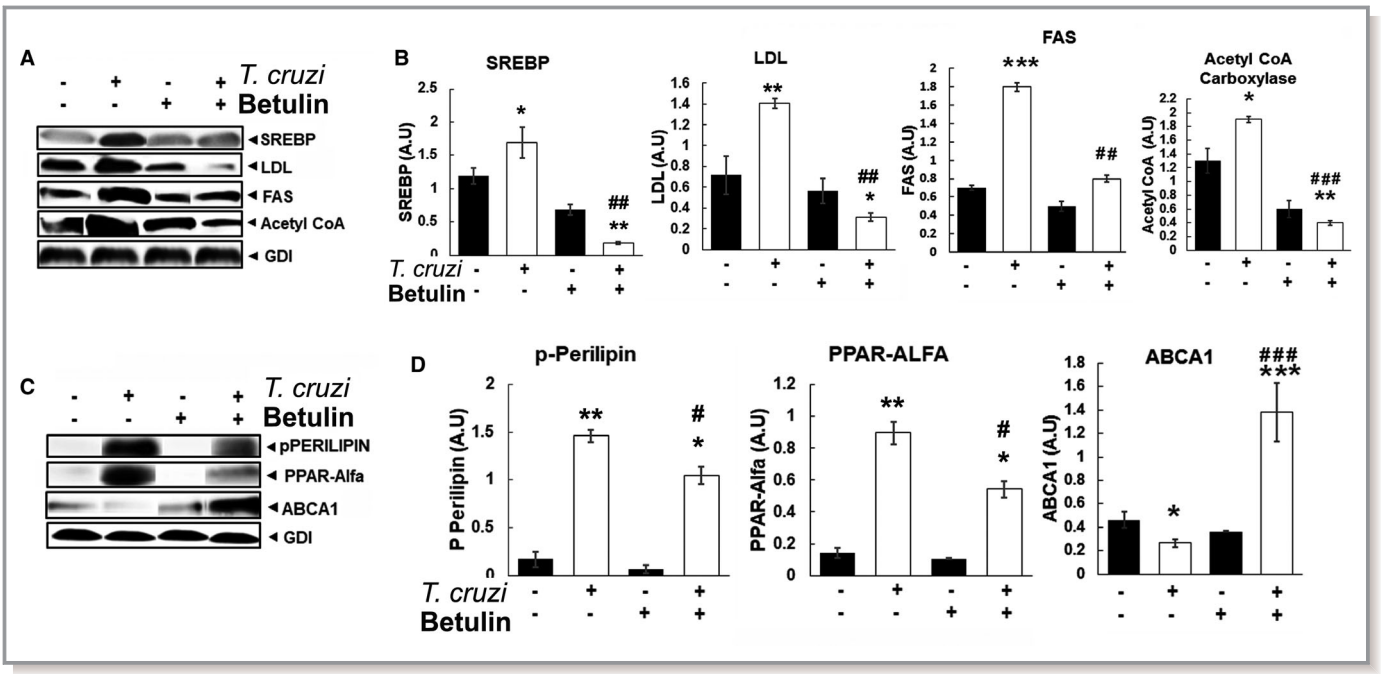

Figure 4. Treatment with SREBP (sterol regulatory element-binding protein) inhibitor increases cardiac cholesterol efflux and reduces fatty acid synthesis in chronic *Trypanosoma cruzi*–infected mice. **A**, Immunoblot analysis of SREBP, LDL (low-density lipoprotein), FAS (fatty acid synthase), and acetyl CoA carboxylase proteins in the hearts of infected or uninfected mice treated or not with SREBP inhibitor at 120 days postinfection (DPI). **B**, Bar graph showing fold changes in the protein levels of SREBP, LDL, FAS, and acetyl CoA carboxylase normalized to GDI expression. **C**, Immunoblot analysis of perilipin, PPAR-α (peroxisome proliferator-activated receptor-α), and ABCA1 (ATP-binding cassette transporter) proteins in the hearts of indicated mice at 120 DPI. **D**, Bar graph showing fold changes in the protein levels of perilipin, PPAR-α, and ABCA1 normalized to GDI (guanosine nucleotide dissociation inhibitor) expression. The error bars represent SEM. A.U. indicates arbitrary unit; p-perilipin, phosphorylated perilipin. $^{*}P\leq0.05$, $^{**}P\leq0.01$, or $^{***}P\leq0.001$ compared with uninfected untreated. $^{\#}P\leq0.05$, $^{\#\#}P\leq0.01$, or $^{\#\#\#}P\leq0.001$ compared with infected untreated.

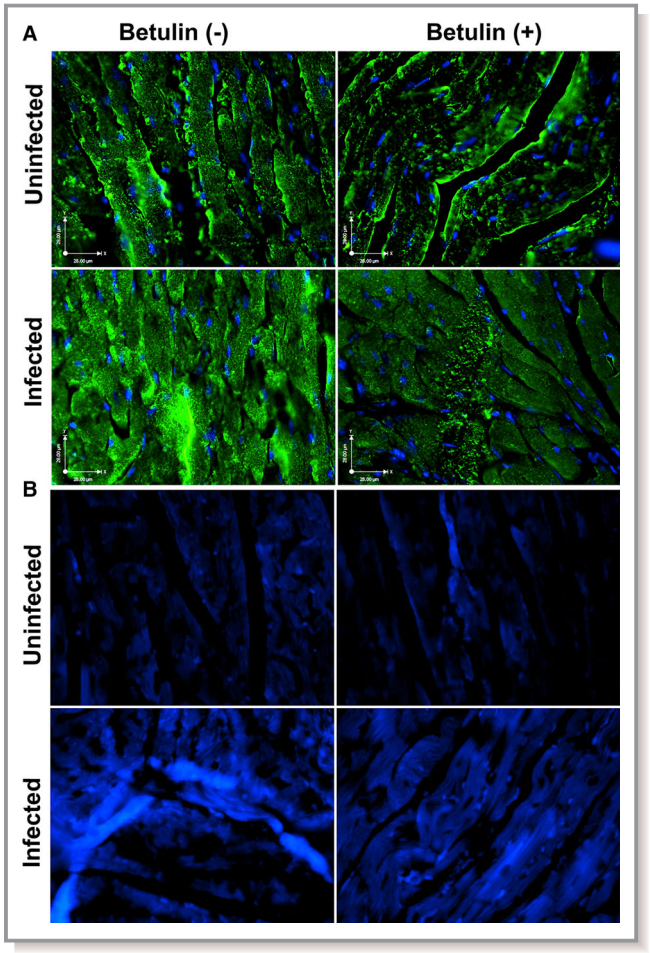

Figure 5. Immunofluorescence and filipin staining of hearts of chronic *Trypanosoma cruzi*–infected mice. **A**, Immunofluorescence analysis of low-density lipoprotein (LDL) on cardiac tissue showing the levels of LDL in the hearts of indicated mice at 120 days postinfection (DPI). **B**, Filipin staining of cholesterol in the hearts of indicated mice at 120 DPI.

uninfected mice at 120 DPI (Figure 6B), which were significantly reduced by treatment with betulin (1.8- and 2-fold, respectively) (Figure 6B). Increased ER stress was associated with inflammation in the hearts of infected mice, as demonstrated by immunoblotting analysis of interferon-γ and TNF-α, which were significantly increased (2- and 4-fold, respectively) compared with uninfected mice at 120 DPI (Figure 6B). This was significantly reduced in infected mice fed a betulin diet by 2- and 1.5-fold, respectively, compared with untreated infected mice (Figure 6B). These data were complemented by qPCR analysis of interferon-γ and TNF-α mRNA levels in the hearts of infected mice treated with and without betulin diet and compared with uninfected untreated mice (Figure 6C). The cardiac mRNA levels of ER stress–related genes BIP, CHOP, and PDI and the inflammatory genes interferon-γ and TNF-α were significantly increased in infected mice and significantly decreased in infected betulin-treated mice compared with uninfected untreated mice (Figure 6C). These data suggest that inhibition of SREBP activation reduces ER stress and inflammation in the hearts of chronically *T cruzi*–infected mice.

Inhibition of SREBP Activation During the Indeterminate Stage of Infection Modulates the Abnormal Levels of Protein Biomarkers of the Cardiac Autonomic Nervous System

Tyrosine hydroxylase and choline acetyltransferase are involved in the sympathetic and parasympathetic signaling of autonomic nervous system.[11,12] The cardiac levels of these biomarkers increase during certain pathological conditions of the heart (eg, in cardiomyopathic Syrian hamsters).[12,13] Immunoblot analysis demonstrated a significant increase in the levels of protein biomarkers (namely, tyrosine hydroxylase and choline acetyltransferase in the hearts of *T cruzi*–infected mice) compared with uninfected mice (Figure 7). In contrast, infected mice fed a betulin diet displayed significantly decreased cardiac levels of tyrosine hydroxylase and choline acetyltransferase compared with untreated mice at 120 DPI, suggesting that inhibition of SREBP activation improves cardiac neurological functions.

Discussion

CCM is the major cause of death and debility in Latin America.[14] The pathogenesis of CCM is multifactorial, and the factors responsible for the transition from the asymptomatic to symptomatic CCM stage are not fully understood. Many primary mechanisms, including the parasite-driven immune response, deregulated cardiac lipid metabolism, mitochondrial dysfunction, and autoreactivity triggered by the infection; and secondary mechanisms, including neurogenic disturbances and coronary microvascular dysfunctions, are likely to determine the outcome of CCM.[15–17] Previously, we demonstrated significant accumulation of lipids in the myocardium, which could induce ER stress.[2,3] We also showed that inhibition of cardiac ER stress improves cardiac morphological characteristics and functions in chronic Chagas mice.[3] The current study analyzed the pathways that induce cardiac lipidopathy and the effect of inhibition of de novo lipid biosynthesis on CCM pathological condition using *T cruzi*–infected CD1 mice as a murine model of Chagas disease. Our data demonstrated that *T cruzi* infection induces cardiac lipid accumulation via SREBP activation, which can be reduced by inhibition of SREBP processing by betulin. We also demonstrated that inhibiting SREBP activation reduces ER stress, inflammation, and neurogenic disturbances in the hearts of *T cruzi*–infected mice and modulates cardiac morphological characteristics

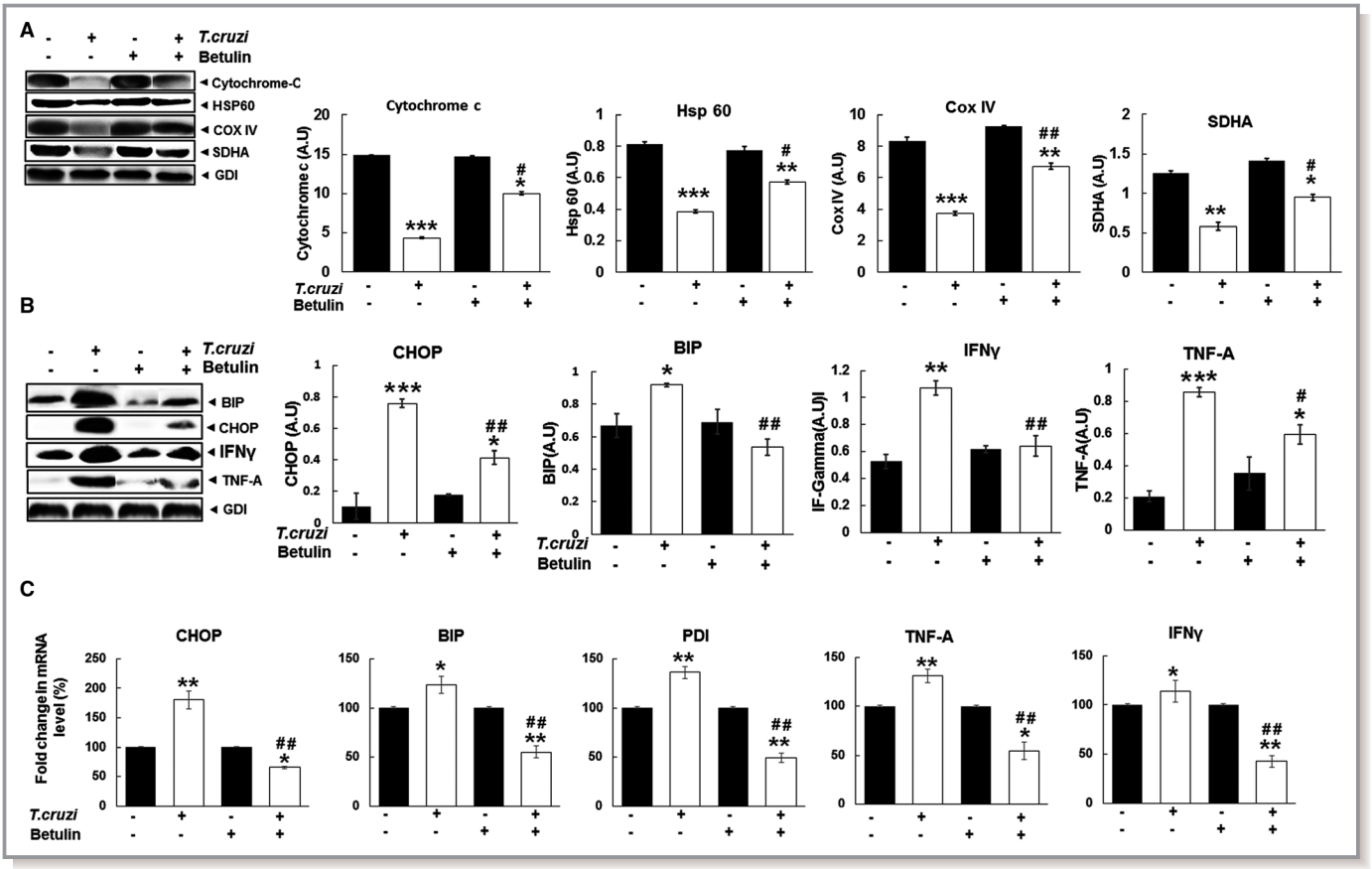

Figure 6. SREBP (sterol regulatory element-binding protein) inhibitor increases protein markers of cardiac mitochondrial function and modulates endoplasmic reticulum stress and inflammation in chronic *Trypanosoma cruzi*–infected mice. **A**, Immunoblot analysis of cytochrome C, HSP (heat shock protein) 60, COX IV (cytochrome oxidase IV), and SDHA (succinate dehydrogenase) proteins in the hearts of indicated mice at 120 days postinfection (DPI). Bar graph depicts fold changes in the protein levels of cytochrome C, HSP-60, COX IV, and SDHA normalized to GDI expression. **B**, Immunoblot analysis of BIP (binding immunoglobulin protein), CHOP (CCAAT-enhancer–binding protein), interferon (IFN)-γ, and tumor necrosis factor (TNF)-α in the hearts of indicated mice at 120 DPI. Bar graph depicts fold changes in the protein levels of BIP, CHOP, IFN-γ, and TNF-α normalized to GDI (guanosine nucleotide dissociation inhibitor) expression. **C**, Quantitative polymerase chain reaction analysis of CHOP, BIP, PDI (protein disulfide isomerase), TNF-α, and IFN-γ mRNA levels in the hearts of indicated mice at 120 DPI. The error bars represent SEM. A.U. indicates arbitrary unit. $^{*}P\leq0.05$ $^{**}P\leq0.01$, or $^{***}P\leq0.001$ compared with uninfected untreated. $^{\#}P\leq0.05$, $^{\#\#}P\leq0.01$ compared with infected untreated.

and ventricular functions. The major limitation of the study is that betulin may affect hepatic lipid metabolism and systemic lipid levels. We also believe that the mouse CD models have their own limitations in the context of translating these results to human CD patients because the serum lipid profiles differ between mouse and humans. Therefore, we suggest that inhibiting SREBP per se may not be a valid strategy. Instead, targeting SREBP inhibitors to the heart and/or finding more specific downstream targets to reduce cardiac lipid accumulation are valuable future strategies to pursue. We state that multifactors are likely involved and that our mouse model "allows" us to study these likely secondary (supporting) causes of CD progression without the confounding effects of parasitemia and inflammation.

SREBPs are major transcription factors activating the expression of genes involved in the biosynthesis of lipids (cholesterol, fatty acid, and triglyceride). SREBPs are synthesized as inactive precursors.[18] Maturation and activation of SREBPs (processing) are under the tight regulatory control of intracellular sterol levels. Unactivated SREBPs bind to the ER membranes through a tight association with cholesterol-sensing protein SCAP and Insig1. Low levels of intracellular sterols dissociate SCAP from Insig, and the released SCAP then escorts the SREBP precursors from the ER to the Golgi, where SREBP undergoes proteolytic cleavage and maturation.[19] Mature SREBP then migrates to the nucleus, where it activates transcription of target genes (lipid biosynthesis). The myocardiums of *T cruzi*–infected mice were overloaded with lipids during the early indeterminate stage and, hence, lower levels of SREBP activation were expected during the indeterminate stage.[3,10] However, we observed significantly greater levels of SREBP and lipid biosynthesis in the hearts of infected

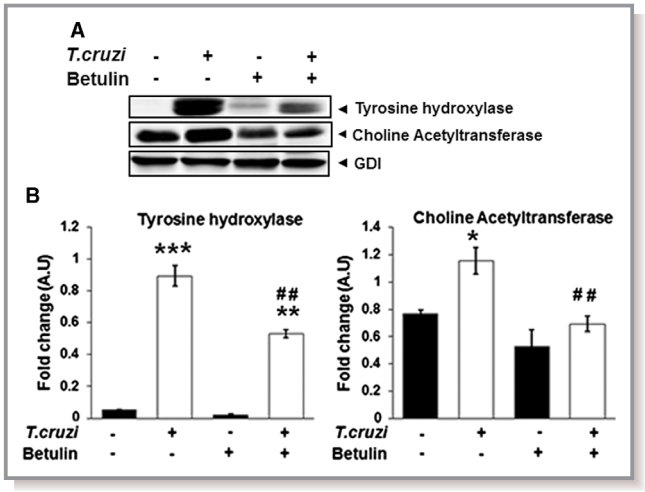

Figure 7. SREBP (sterol regulatory element-binding protein) inhibitor modulates the levels of protein markers of the cardiac autonomic nervous system in chronic *Trypanosoma cruzi*–infected mice. **A**, Immunoblot analysis of tyrosine hydroxylase and choline acetyltransferase proteins in the hearts of indicated mice at 120 days postinfection. **B**, Bar graph depicts fold changes in the protein levels of tyrosine hydroxylase and choline acetyltransferase normalized to GDI (guanosine nucleotide dissociation inhibitor) expression. The error bars represent SEM. A.U. indicates arbitrary unit. $^{**}P \leq 0.01$ compared with uninfected untreated. $^{\#}P \leq 0.05$, $^{\#\#}P \leq 0.01$, or $^{\#\#\#}P \leq 0.001$ compared with infected untreated.

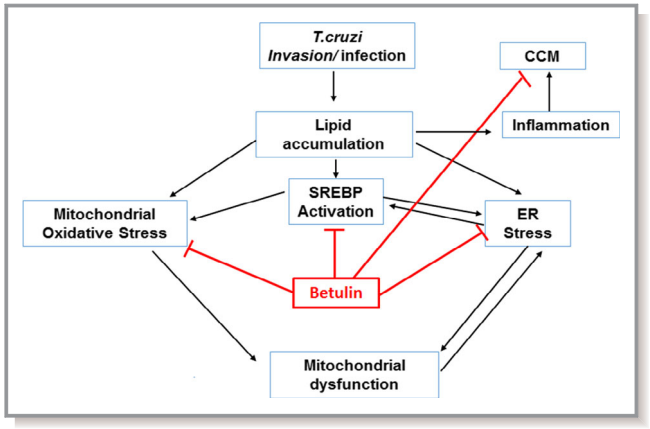

Figure 8. A schematic representation of the modulatory effect of betulin in the pathogenesis of Chagas cardiomyopathy (CCM). *Trypanosoma cruzi* infection increases cardiac lipid accumulation and SREBP (sterol regulatory element-binding protein) activation during indeterminate stage of infection in murine CD models. Induction and consequence of SREBP activation causes increased mitochondrial oxidative stress and endoplasmic reticulum (ER) stress and results in mitochondrial dysfunction, a major cause of cardiac pathogenesis in Chagas disease. Inhibition of SREBP activation decreases mitochondrial oxidative stress and ER stress and modulates cardiac physiological characteristics.

mice compared with uninfected mice during indeterminate and chronic stages of infection (Figure 4). This is likely because of increased cardiac PPAR-α levels, which could induce SREBP activation,[20] leading to excessive intracellular lipid levels. Thus, we propose that these elevated cardiac lipids induce mitochondrial oxidative stress and ER stress (Figure 8) and form a vicious cycle of lipid biosynthesis–mitochondrial and ER stress, resulting in ventricular dysfunction (Figure 8). We hypothesized that inhibiting SREBP processing could dissect this vicious cycle and thereby modulate ventricular functions in *T cruzi*–infected mice during chronic infection (Figure 8).

Earlier studies have shown beneficial effects of betulin in *T cruzi* infection as a parasitic drug and an anti-inflammatory agent.[21,22] Betulin has been used to reduce intracellular lipid levels in many animal studies.[23] Our in vitro studies also confirmed that betulin reduces de novo fatty acid and cholesterol biosynthesis (Figure 1) and results in decreased ER stress in *T cruzi*–infected cultured cardiomyocytes (Figure 2). *T cruzi*–infected CD1 mice supplemented with betulin showed a significant reduction in SREBP transcription, expression, maturation, and activation. Decreased SREBP maturation and activation during the indeterminate stage reduced the accumulation of intracellular lipids in the myocardium. Increased intracellular lipid levels elevate cardiac lipid lipolysis and fatty acid oxidation, which resulted in cardiac mitochondrial dysfunction, as indicated by the decreased levels of cytochrome C, HSP-60, COX IV, and SDHA (Figure 6A). Cytochrome C, COX IV, and SDHA are part of the electron transport chain and play a significant role in energy biosynthesis from β-oxidation.[24] Intracellular lipids generally increase the levels of these β-oxidation marker proteins.[25] However, although the lipid levels were significantly increased in the hearts of *T cruzi*–infected mice, the levels of β-oxidation marker proteins were reduced, indicating that the accumulated lipids were not completely oxidized in the hearts during chronic infection. Thus, increased intracellular lipids could lead to ER stress, which our data support. Altogether, our data suggest that inhibition of excess lipid biosynthesis in the myocardium during chronic *T cruzi* infection inhibits mitochondrial dysfunction and modulates ER stress and, thus, prevents excessive accumulation of lipids and lipotoxicity.

Cardiac ER stress could lead to myocardial inflammation and cell death and result in fibrosis.[26] Significant myocardial cell death and fibrosis alter ventricular anatomical characteristics and hinder the ventricular capacity to pump the blood, leading to cardiac dilation. Betulin treatment also improved cardiac pathological characteristics, as demonstrated by modulated inflammation and fibrosis compared with untreated infected mice. We also demonstrated that betulin treatment modulates cardiac neurodysfunctions by modulating the levels of autonomic nervous system signaling markers. Our data demonstrated that betulin treatment successfully

breaks the vicious cycle between deregulated de novo lipid biosynthesis and ER stress, improves cardiac morphological characteristics and ventricular anatomical characteristics, and modulates CCM in murine chronic Chagas disease model. These studies provide evidence to support the design of new drugs to inhibit cardiac lipid biosynthesis and lipid accumulation to potentially prevent the development and progression of CCM. On the basis of our data, we conclude that therapeutic drugs targeting the inhibition of pathways that trigger deregulated lipid biosynthesis and accumulation of lipids in the heart at the early stage of chronic infection may be an effective strategy to prevent the progression of CCM.

Acknowledgments

We thank members of the Rutgers Imaging Center and Histology Core Facility for their assistance with tissue collection, histological analysis, and image acquisition. We acknowledge the editorial assistance of the Life Science Editors.

Sources of Funding

This study was supported by grants from the National Heart, Lung, and Blood Institute (National Institutes of Health HL-122866) to Dr Nagajyothi.

Disclosures

None.

References

1. Machado FS, Tanowitz HB, Ribeiro AL. Pathogenesis of Chagas cardiomyopathy: role of inflammation and oxidative stress. *J Am Heart Assoc*. 2013;2:e000539. DOI: 10.1161/JAHA.113.000539.
2. Johndrow C, Nelson R, Tanowitz H, Weiss LM, Nagajyothi F. *Trypanosoma cruzi* infection results in an increase in intracellular cholesterol. *Microbes Infect*. 2014;4:337–344.
3. Janeesh PA, Lizardo K, Wang S, Yurkow E, Nagajyothi JF. Inhibition of ER stress by 2-aminopurine treatment modulates cardiomyopathy in a murine chronic Chagas disease model. *Biomol Ther*. 2019;27:386–394.
4. Colgan SM, Tang D, Werstuck GH, Austin RC. Endoplasmic reticulum stress causes the activation of sterol regulatory element binding protein-2. *Int J Biochem Cell Biol*. 2007;39:1843–1851.
5. Crunkhorn S. Metabolic disease: birch bark compound combats metabolic syndrome. *Nat Rev Drug Discovery*. 2011;3:175.
6. Bustamante JM, Rivarola HW, Fernández AR, Enders JE, Fretes R, Palma JA, Paglini-Oliva PA. Indeterminate Chagas' disease: *Trypanosoma cruzi* strain and re-infection are factors involved in the progression of cardiopathy. *Clin Sci*. 2003;104:415–420.
7. Khare S, Liu X, Stinson M, Rivera I, Groessl T, Tuntland T, Yeh V, Wen B, Molteni V, Glynne R, Supek F. Antitrypanosomal treatment with benznidazole is superior to posaconazole regimens in mouse models of Chagas disease. *Antimicrob Agents Chemother*. 2015;59:6385–6394.
8. Combs TP, Nagajyothi F, Mukherjee S, de Almeida CJ, Jelicks LA, Schubert W, Lin Y, Jayabalan DS, Zhao D, Braunstein VL, Landskroner-Eiger S, Cordero A, Factor SM, Weiss LM, Lisanti MP, Tanowitz HB, Scherer PE. The adipocyte as an important target cell for *Trypanosoma cruzi* infection. *J Biol Chem*. 2005;280:24085–24094.
9. Nagajyothi F, Weiss LM, Zhao D, Koba W, Jelicks LA, Cui MH, Factor SM, Scherer PE, Tanowitz HB. High fat diet modulates *Trypanosoma cruzi* infection associated myocarditis. *PLoS Negl Trop Dis*. 2014;8:p.e3118.
10. Nagajyothi F, Weiss LM, Silver DL, Desruisseaux MS, Scherer PE, Herz J, Tanowitz HB. *Trypanosoma cruzi* utilizes the host low density lipoprotein receptor in invasion. *PLoS Negl Trop Dis*. 2011;5:e953.
11. Lund DD, Knuepfer MM, Brody MJ, Bhatnagar RK, Schmid PG, Roskoski R Jr. Comparison of tyrosine hydroxylase and choline acetyltransferase activity in response to sympathetic nervous system activation. *Brain Res*. 1978;156:192–197.
12. Lund DD, Schmid PG, Davis JA, Sharabi FM, Roskoski R Jr. Increased choline acetyltransferase activity in pressure-overloaded right ventricles of guinea pigs. *Life Sci*. 1983;32:2257–2264.
13. Sole MJ, Wurtman RJ, Lo CM, Kamble AB, Sonnenblick EH. Tyrosine hydroxylase activity in the heart of the cardiomyopathic Syrian hamster. *J Mol Cell Cardiol*. 1977;9:225–233.
14. Guillermo M. Chagas cardiomyopathy. E-Journal of Cardiol. *Pract.-Eur. Soc. Cardiol*. 2016;14:31.
15. Nunes MC, Beaton A, Acquatella H, Bern C, Bolger AF, Echeverria LE, Dutra WO, Gascon J, Morillo CA, Oliveira-Filho J, Ribeiro AL. Chagas cardiomyopathy: an update of current clinical knowledge and management: a scientific statement from the American Heart Association. *Circulation*. 2018;138:169–209.
16. Machado FS, Dutra WO, Esper L, Gollob KJ, Teixeira MM, Factor SM, Weiss LM, Nagajyothi F, Tanowitz HB, Garg NJ. Current understanding of immunity to *Trypanosoma cruzi* infection and pathogenesis of Chagas disease. *Semin Immunopathol*. 2012;34:753–770.
17. Tanowitz HB, Machado FS, Spray DC, Friedman JM, Weiss OS, Lora JN, Nagajyothi J, Moraes DN, Garg NJ, Nunes MC, Ribeiro AL. Developments in the management of Chagas cardiomyopathy. *Expert Rev Cardiovasc Ther*. 2015;13:1393–1409.
18. Horton JD, Goldstein JL, Brown MS. SREBPs: activators of the complete program of cholesterol and fatty acid synthesis in the liver. *J Clin Invest*. 2002;109:1125–1131.
19. Ye J, DeBose-Boyd RA. Regulation of cholesterol and fatty acid synthesis. *Cold Spring Harb Perspect Biol*. 2011;3:a004754.
20. Yan F, Wang Q, Xu C, Cao M, Zhou X, Wang T, Yu C, Jing F, Chen W, Gao L, Zhao J. Peroxisome proliferator-activated receptor α activation induces hepatic steatosis, suggesting an adverse effect. *PLoS One*. 2014;9:e99245.
21. Sousa PL, da Silva Souza RO, Tessarolo LD, Sampaio TL, Canuto JA, Martins AM. Betulinic acid induces cell death by necrosis in *Trypanosoma cruzi*. *Acta Trop*. 2017;174:72–75.
22. Meira CS, Santos ED, do Espírito Santo RF, Vasconcelos JF, Orge ID, Nonaka CK, Barreto BC, Caria AC, Silva DN, Barbosa-Filho JM, Macambira SG. Betulinic acid derivative BA5, attenuates inflammation and fibrosis in experimental chronic Chagas disease cardiomyopathy by inducing IL-10 and M2 polarization. *Front Immunol*. 2019;10:1257.
23. Tang JJ, Li JG, Qi W, Qiu WW, Li PS, Li BL, Song BL. Inhibition of SREBP by a small molecule, betulin, improves hyperlipidemia and insulin resistance and reduces atherosclerotic plaques. *Cell Metab*. 2011;13:44–56.
24. Signes A, Fernandez-Vizarra E. Assembly of mammalian oxidative phosphorylation complexes I-V and supercomplexes. *Essays Biochem*. 2018;62:255–270.
25. Turner N, Bruce CR, Beale SM, Hoehn KL, So T, Rolph MS, Cooney GJ. Excess lipid availability increases mitochondrial fatty acid oxidative capacity in muscle: evidence against a role for reduced fatty acid oxidation in lipid-induced insulin resistance in rodents. *Diabetes*. 2007;56:2085–2092.
26. Luo T, Kim JK, Chen B, Abdel-Latif A, Kitakaze M, Yan L. Attenuation of ER stress prevents post-infarction-induced cardiac rupture and remodeling by modulating both cardiac apoptosis and fibrosis. *Chem Biol Interact*. 2015;225:90–98.

Supplemental Material

Figure S1. Schematic representation of the experimental design of the in *vivo* (a) and in *vitro* (b) studies.

a. Experimental design of *in vivo* studies

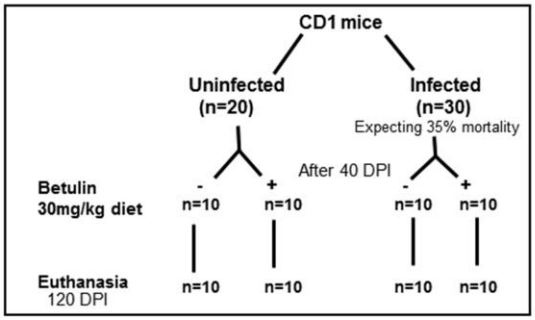

b. Experimental design of *in vitro studies*

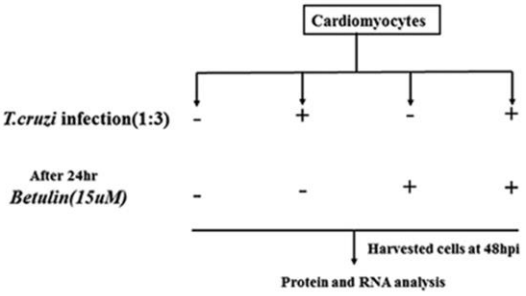

Figure S2. Effect of sterol regulatory element-binding protein (SREBP) inhibitor (Betulin) on SREBP signaling, adipokine, fatty acid and cholesterol metabolism in cardiomyocytes infected with *T.cruzi.*

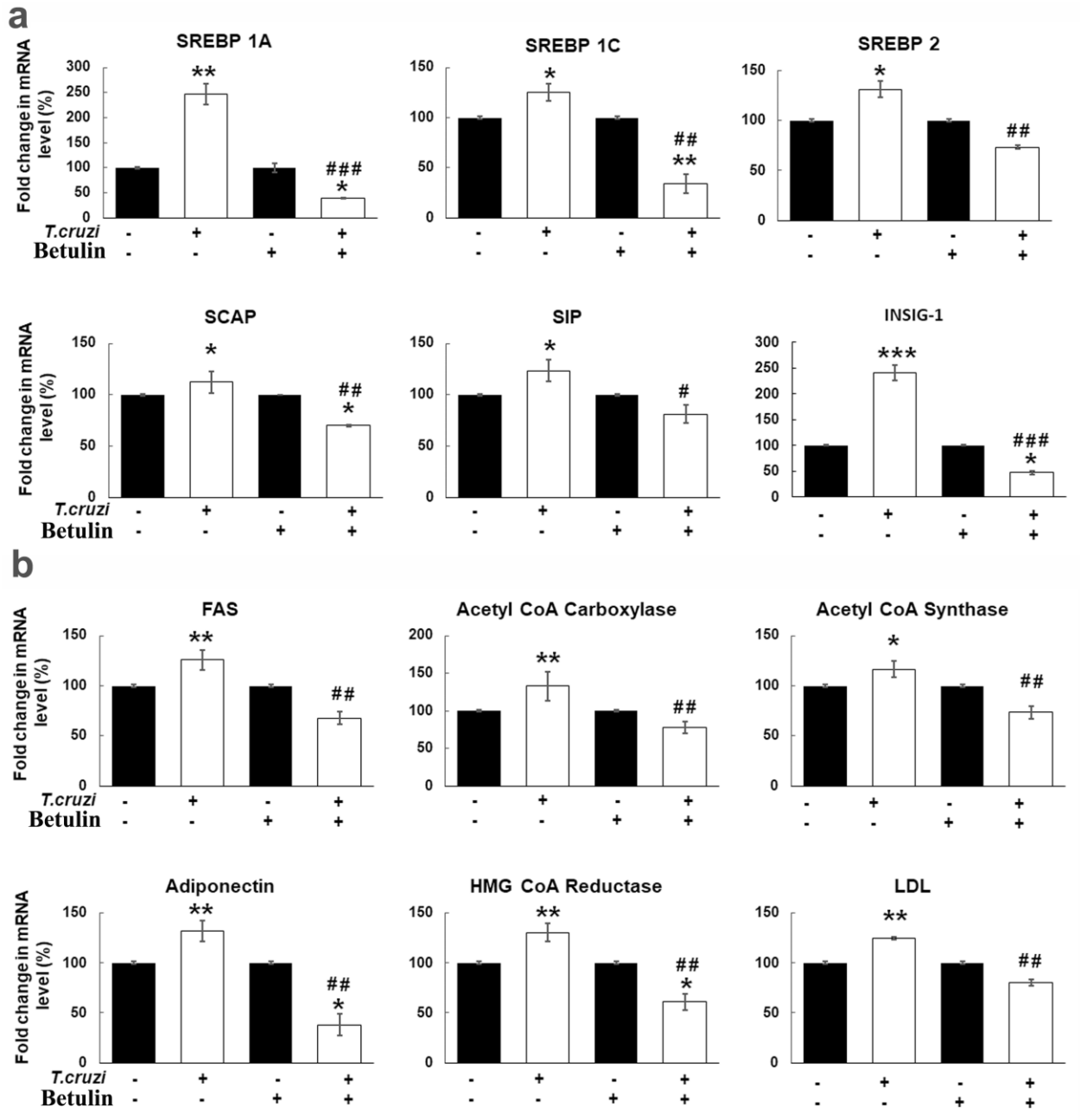

(a) qPCR analysis of SREBP-1A, SREBP-1C, SREBP-2, SCAP, SIP, and INSIG-1 mRNA levels in infected or uninfected H9c2 cells treated or not with SREBP inhibitor.

(b) qPCR analysis of FAS, acetyl CoA carboxylase, acetyl CoA synthase, adiponectin HMG-CoA and LDL mRNA levels in H9c2 cells under the indicated conditions.

The error bars represent standard error of the mean. * $p \leq 0.05$, ** $p \leq 0.01$ or *** $p \leq 0.001$ compared to uninfected untreated. # $p \leq 0.05$, ## $p \leq 0.01$ or ### $p \leq 0.001$compared to infected untreated.

Figure S3. Effect of sterol regulatory element-binding protein (SREBP) inhibitor (Betulin) on SREBP signaling, fatty acid synthesis genes and cholesterol metabolism in the hearts of chronic *T. cruzi* infected mice.

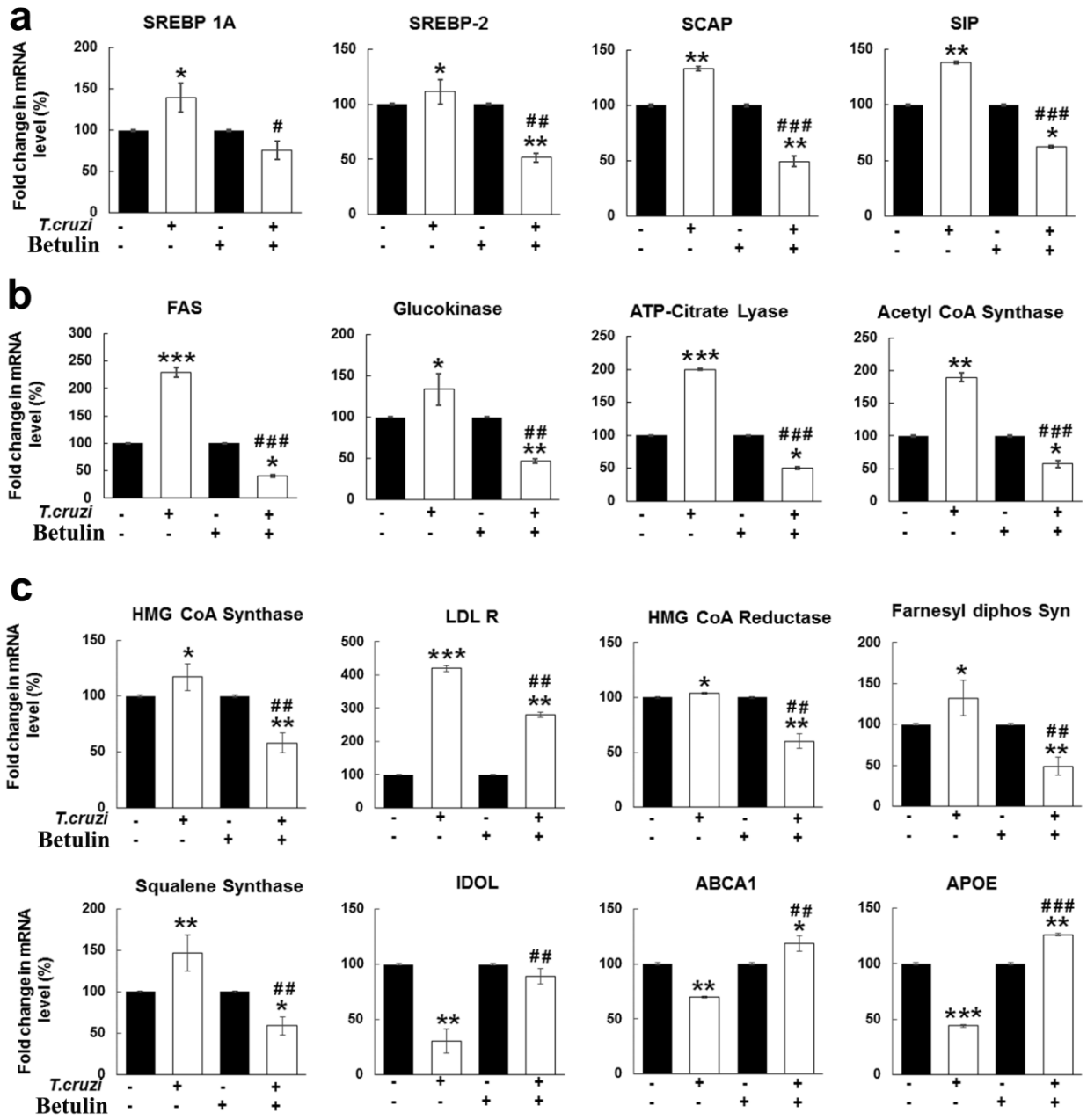

(a) qPCR analysis of SREBP 1A, SREBP 2, SCAP and SIP mRNA levels in the hearts of indicated mice at 120DPI.

(b) qPCR analysis of FAS, glucokinase, ATP citrate lyase and acetyl CoA synthase mRNA levels in the hearts of indicated mice at 120DPI.

(c) qPCR analysis of HMG-CoA synthase, LDL-R, HMG- CoA reductase, farnesyl diphosphate synthase, squalene synthase, ABCA1, IDOL and APOE mRNA levels in indicated mice at 120DPI.

The error bars represent standard error of the mean. * $p \leq 0.05$, ** $p \leq 0.01$ or *** $p \leq 0.001$ compared to uninfected untreated. # $p \leq 0.05$, ## $p \leq 0.01$ or ### $p \leq 0.001$compared to infected untreated.